Folia Neuropathologica

# Clustering and periodicity of neurofibrillary tangles in the upper and lower cortical laminae in Alzheimer's disease

Richard A. Armstrong

Vision Sciences, Aston University, Birmingham, UK

*Folia Neuropathol 2008; 46 (1): 26-31*

## Abstract

*In Alzheimer's disease (AD), neurofibrillary tangles (NFT) occur within neurons in both the upper and lower cortical laminae. Using a statistical method that estimates the size and spacing of NFT clusters along the cortex parallel to the pia mater, two hypotheses were tested: 1) that the cluster size and distribution of the NFT in gyri of the temporal lobe reflect degeneration of the feedforward (FF) and feedback (FB) cortico-cortical pathways, and 2) that there is a spatial relationship between the clusters of NFT in the upper and lower laminae. In 16 temporal lobe gyri from 10 cases of sporadic AD, NFT were present in both the upper and lower laminae in 11/16 (69%) gyri and in either the upper or lower laminae in 5/16 (31%) gyri. Clustering of the NFT was observed in all gyri. A significant peak-to-peak distance was observed in the upper laminae in 13/15 (87%) gyri and in the lower laminae in 8/12 (67%) gyri, suggesting a regularly repeating pattern of NFT clusters along the cortex. The regularly distributed clusters of NFT were between 500 and 800 µm in size, the estimated size of the cells of origin of the FF and FB cortico-cortical projections, in the upper laminae of 6/13 (46%) gyri and in the lower laminae of 2/8 (25%) gyri. Clusters of NFT in the upper laminae were spatially correlated (in phase) with those in the lower laminae in 5/16 (31%) gyri. The clustering patterns of the NFT are consistent with their formation in relation to the FF and FB cortico-cortical pathways. In most gyri, NFT clusters appeared to develop independently in the upper and lower laminae.*

***Key words:*** *Alzheimer's disease, neurofibrillary tangles, pattern analysis by regression, clustering, cortico-cortico projections, peak-to-peak distance.*

## Introduction

In the cerebral cortex in Alzheimer's disease (AD), neurofibrillary tangles (NFT) occur within the larger pyramidal neurons in both the upper and lower cortical laminae [12,15,21,22,26]. These results suggest that NFT affect both the feedforward (FF) and feedback (FB) cortico-cortical pathways which have their cells of origin mainly in laminae II/III and V/VI respectively [15] and that NFT pathology could spread between cortical areas via these projections [28]. Consistent with this hypothesis, NFT in the cerebral cortex are often clustered [20,26], the clusters being regularly distributed along the cortex parallel to the pia mater [1,3]. If NFT are related to

**Communicating author:**

Richard A. Armstrong, Vision Sciences, Aston University, Birmingham B4 7ET, U.K., tel.: +44 121 204 41 02, fax: +44 121 204 40 48, Email: R.A.Armstrong@aston.ac.uk

the FF and FB pathways, there should be a pattern of regularly repeating NFT clusters of similar size to the cells of origin of the cortico-cortical pathways, estimated to be between 500 and 800 µm [20].

In addition, NFT could spread across the cortex within vertical columns of cells since cortical columns associated with these projections are heavily interconnected along the vertical axis but sparsely in the horizontal plane [24]. If spread of NFT occurs within a column then there should be a spatial correlation between the NFT clusters in the upper and lower laminae.

Previous methods of measuring the spatial patterns of NFT [1,3,6,26] have used the 'Poisson' method to estimate cluster size. This method, however, does not measure the cluster size accurately and does not provide an estimate of the spacing or 'periodicity' of the clusters [2]. Hence, the Poisson method has limited usefulness in testing specific hypotheses relating NFT distribution to anatomical projections. Pattern analysis by regression [4], however, provides a more accurate estimate of cluster size and a measure of the spacing of the clusters. Using this method, two hypotheses were tested: 1) that the spatial arrangement and cluster size of the NFT is consistent with degeneration of the FF and FB cortico-cortical pathways, and 2) that there is a spatial relationship between clusters of NFT in the upper and lower laminae consistent with spread of NFT within vertical columns of cells.

## Materials and Methods

### Cases

Ten cases of sporadic AD (details in Table I) were obtained from the Brain Bank, Department of Neuropathology, Institute of Psychiatry. Informed consent was given for the removal of all tissue and followed the principles embodied in the 1964 Helsinki declaration (as modified Edinburgh, 2000). Post-mortem (PM) delay was less than 20 hours in each case. The AD cases were clinically assessed and all fulfilled the 'National Institute of Neurological and Communicative Disorders and Stroke and Alzheimer's Disease and Related Disorders Association' (NINCDS/ADRDA) criteria for probable AD [29]. The histological diagnosis of AD was established by the presence of widespread neocortical senile plaques (SP) consistent with the 'Consortium to Establish a Registry of Alzheimer's Disease' (CERAD) criteria [25]. In addition, NFT were abundant in the cerebral cortex and hippocampus of each case.

### Tissue preparation

Blocks of the temporal cortex, including the inferior temporal gyrus (ITG) and parahippocampal gyrus (PHG), were taken from each case at the level of the lateral geniculate body. Tissue was fixed in 10% phosphate buffered formal-saline and embedded in paraffin wax. 7 µm coronal sections were stained with the Gallyas silver impregnation method [18], which reveals the cellular NFT particularly clearly [10]. Sections were counterstained with haematoxylin to reveal the neuronal and glial cytoarchitecture.

### Morphometric methods

Laminae II/III and V/VI contain the majority of pyramidal cells that give rise to the FF and FB projections respectively [16,17,30] and the majority of NFT in AD are associated with these laminae [14,21,23,27]. Hence, in each gyrus with sufficient densities of NFT, two guidelines were marked on the slide, one at the lamina I/II boundary to sample laminae II/III and one at the IV/V boundary to sample laminae V/VI. NFT were counted in horizontal strips of tissue using between 64 and 128 contiguous 125 × 250 µm microscopic fields, the short dimension of the sample field being aligned parallel to the appropriate guideline.

**Table I.** Demographic data and cause of death of the cases studied

| Patient | Gender | Age | Onset | Cause of death |
|---|---|---|---|---|
| A | M | 82 | 78 | bronchopneumonia |
| B | M | 73 | 66 | bronchopneumonia |
| C | F | 87 | 82 | myocardial infarction |
| D | F | 82 | 75 | bronchopneumonia |
| E | F | 66 | 59 | NA |
| F | F | 70 | 64 | bronchopneumonia |
| G | F | 85 | 80 | bronchopneumonia |
| H | F | 70 | NA | ischaemic heart disease |
| I | M | 80 | 77 | bronchopneumonia |
| J | M | 88 | 72 | bronchopneumonia |

*M – male, F – female, NA – data not available*

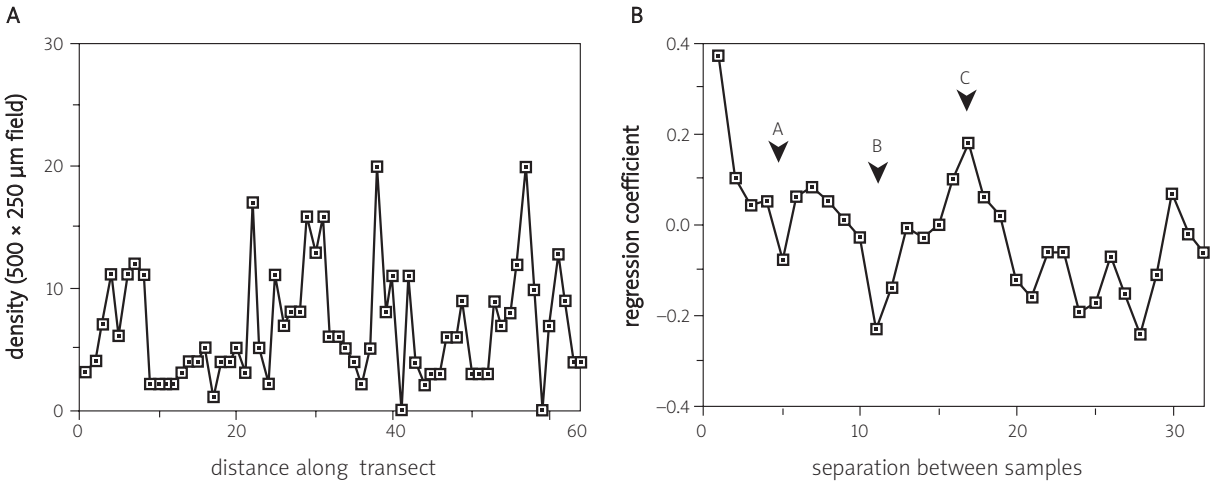


**Fig. 1A-B.** Spatial pattern analysis by regression of neurofibrillary tangles (NFT) along the inferior temporal gyrus of patient A: A) Density plot showing variation in the numbers of NFT along the cortex, B) pattern analysis plot of the density data. Arrows A and B indicate $-\beta_{max}$, the cluster sizes present, and arrow C indicates $+\beta_{max}$, the peak-to-peak distance

## Spatial pattern analysis

The data were analysed using 'pattern analysis by regression' [4,13]. The method is based on the principle that if the NFT are clustered along the cortex, densities in adjacent sample fields (comprising the X and Y variables) will both be high if the fields are located over a cluster and low if they are located between two clusters. In such a case, adjacent pairs of values taken from all of the contiguous fields will be positively correlated as measured by the linear regression coefficient (β). If the spacing between the sample fields is increased, i.e. the sample fields are separated by one field, two fields, etc., it becomes increasingly probable that there will be pairs of values such that one member of the pair will be located over a cluster of NFT and the other over an adjacent space. Hence, the value of β will decrease as the degree of separation between the pairs of sample fields increases. The degree of spacing at which the maximum significant negative regression coefficient ($-\beta_{max}$) occurs is an estimate of the mean cluster size [4]. In addition, if clusters are distributed more or less evenly along the strip of tissue sampled, a significant $+\beta_{max}$ indicates the peak-to-peak distance of the clusters of NFT. This is because at greater degrees of separation, the sample fields are now so widely spaced that they span adjacent clusters or spaces. Hence, β is calculated for pairs of adjacent fields and then with an increasing degree of separation (i.e. separated by 1, 2, 3, 4, 5, ....., n units). β is plotted as a function of the degree of separation between the sample fields and the significance of β determined by a 't' test of the regression coefficient [4].

To determine the spatial correlation between the clusters of NFT in the upper and lower laminae, the degree of correlation between the NFT densities was tested using Pearson's correlation coefficient ('r') [5]. The degree of spatial correlation depends on the field size at which densities are measured [5]. Hence, adjacent lesion densities were added together successively in pairs to create larger field sizes, viz., 125 × 250 µm, 250 × 250 µm, 500 × 250 µm, etc., up to a size limited by the number of original sample fields. Pearson's 'r' was calculated between the densities at each field size to establish the scale at which the correlation was most evident. Significant correlations present at the smallest field size suggests a close spatial relationship between the lesions at field sizes less than 250 × 250 µm, whereas correlations present at larger scales only, e.g. 500 × 250 µm or 1000 × 250 µm, could be due to the general abundance of NFT in the upper and lower cortex [5].

## Results

An example of a pattern analysis plot using the regression method (ITG, upper laminae of Patient A) is shown in Fig. 1. The clustering of NFT along the cortical strip is evident from the density plot (Fig. 1A). The

**Table II.** Clustering and periodicity of neurofibrillary tangles (NFT) in the upper and lower cortical laminae in gyri of the temporal lobe in ten patients with sporadic Alzheimer's disease

| Case | Region | Upper cortex | | Lower cortex | |
|---|---|---|---|---|---|
| | | Cluster size (µm) | PD (µm) | Cluster size (µm) | PD (µm) |
| A | ITG | 625, 1375 | 2125 | 5875 | – |
| | PHG | >4000 | 7000 | 2750 | 4750 |
| B | ITG | 1125 | 3750 | 750 | 2500 |
| | PHG | >4000 | – | – | – |
| C | ITG | 1375 | 4750 | 1000 | 3375 |
| | PHG | 750 | 2500 | 1500 | – |
| D | PHG | 625 | 1500 | – | – |
| E | ITG | 250 | 1500 | – | – |
| | PHG | 500 | 1875 | – | – |
| F | PHG | 1125 | 2875 | 1000 | 3375 |
| G | PHG | – | – | 1875 | – |
| H | ITG | 1375 | 4000 | 500 | 1125 |
| | PHG | 500 | 3000 | 1875 | – |
| I | ITG | 250 | 1125 | 1125 | 2375 |
| | PHG | 1625 | 5125 | 1125 | 2375 |
| J | ITG | 875 | – | 1000 | 3250 |

*PD – peak-to-peak distance. Comparison of mean dimensions between upper and lower laminae: cluster size t = 0.70 (P > 0.05); peak-to-peak distance t = 0.41 (P > 0.05); correlations between upper and lower laminae: cluster size r = 0.45 (P > 0.05); peak-to-peak distance r = –0.06 (P > 0.05)*

spatial pattern analysis plot (Fig. 1B) indicates three significant peaks: a negative peak 'A' at a degree of separation of 5 units indicates the presence of clusters of NFT approximately 625 µm in diameter (5 × 125 µm), 2) a negative peak 'B' at a degree of separation of 11 units suggesting aggregation of NFT into larger clusters approximately 1375 µm (11 × 125 µm) in diameter, 3) and a positive peak 'C' at degree of separation of 17 units, indicating that the larger clusters are distributed with a peak-to-peak distance of approximately 2125 µm (17 × 125 µm). There is some evidence that the smaller clusters may also be regularly distributed but the positive peak at a separation distance of 7 units was not significant.

**Table III.** Correlations (Pearson's 'r') between the densities of neurofibrillary tangles (NFT) in the upper and lower cortex in 10 cases of Alzheimer's disease. Data indicate the field sizes (µm) at which there was a significant correlation

| Case | Region | Correlation |
|---|---|---|
| A | ITG | ns |
| | PHG | 125***, 250**, 500***, 1000***, 2000** |
| B | ITG | 125* |
| C | ITG | ns |
| | PHG | ns |
| F | PHG | 500*, 1000* |
| H | ITG | ns |
| | PHG | 800* |
| I | ITG | ns |
| | PHG | 2000* |
| J | ITG | ns |

****P < 0.001; **P < 0.01; *P < 0.05; ns – not significant*

The spatial patterns of the NFT in all 16 gyri studied are shown in Table II. NFT were present in both the upper and lower laminae in 11/16 (69%) gyri, and in either the upper or lower laminae in 5/16 (31%) gyri. Clustering of the NFT was evident in all gyri. A significant peak-to-peak distance was observed in the upper laminae in 13/15 (87%) gyri and in the lower laminae in 8/12 (67%) gyri, suggesting a repeating pattern of NFT clusters along the cortex. Clusters were in the size range 500-800 µm in 6/13 (46%) analyses of the upper cortex and 2/8 (25%) analyses of the lower cortex. In gyri with NFT in the upper and lower laminae, there were no significant laminar differences in cluster size ($t = 0.70$, $P > 0.05$) or peak-to-peak distance ($t = 0.41$, $P > 0.05$). In addition, there were no significant correlations between either the cluster size ($r = 0.45$, $P > 0.05$) or peak-to-peak distance ($r = –0.06$, $P > 0.05$) in the upper laminar compared with corresponding values in the lower laminae.

The spatial correlations between the densities of NFT in the upper and lower cortical laminae are shown in Table III. Variations in the density of NFT in the upper cortex were positively correlated with those in the lower cortex in 5/16 (31%) gyri. In gyri with a significant positive correlation, correlations

were present at the smallest field size in two gyri and at the larger field sizes only in three gyri.

## Discussion

This study examined two hypotheses: 1) that the clustering patterns of NFT in the temporal lobe are attributable to the degeneration of the cells of origin of the FF and FB cortico-cortical projections, and 2) that there was a spatial relationship between the clusters of NFT in the upper and lower cortical laminae. The data provide evidence to support the first hypothesis but less evidence for the second hypothesis.

In primates, the cells of origin of the cortico-cortical projections are clustered and occur in bands that are regularly distributed along the cortex. Individual bands of cells, approximately 500-800 µm in width, traverse the cortical laminae in columns [20]. Hence, if NFT are associated with these cells, they should be distributed in clusters which have a regular periodicity along the cortex, and with a mean size between 500 and 800 µm. In most gyri, the NFT occurred in regularly distributed clusters consistent with the hypothesis [1]. In addition, in 46% of analyses of the upper laminae and 25% of analyses of the lower laminae, the sizes of the NFT clusters were within the predicted range of 500-800 µm [20]. In the remaining gyri, however, the clusters of NFT were either smaller or larger than predicted. A smaller than expected cluster could result from the development of NFT in relation to a subset of neurons within a column. Clustering on a larger scale, e.g. >1000 µm, could be due to a number of factors. First, the larger clusters of NFT may not be related to the cortico-cortical projections as hypothesised but to other anatomical or pathological features of the cortex that exhibit a regular distribution, such as the SP [9,11,19] or blood vessels [7]. However, clusters of NFT do not coincide with those of SP [8,9,11] and there is no evidence that cortical NFT are clustered around blood vessels in AD. Second, the cells of origin of the cortico-cortical projections may be larger than 500-800 µm in some cortical areas. Third, there may be a relationship between the size of NFT clusters and the stage of the disease. Initially, NFT may affect small numbers of neurons within a column but could then spread, first to involve the whole cell cluster, and second to adjacent columns via the intracortical circuits. Consistent with this hypothesis, a positive correlation has been observed between cluster size and density of NFT [1].

Clusters of NFT were in phase in the upper and lower laminae in about a third of the gyri studied. In some of these gyri, however, a significant correlation was present only at larger field sizes (>500 µm), which may reflect the general abundance of NFT in the upper and lower cortex rather than a specific correlation within a column. In the majority of gyri, the NFT clusters appeared to be distributed independently in the upper and lower laminae. The bands of cells that constitute the cortico-cortical pathways form an irregular branching and rejoining pattern across the cortex [20]. Hence, neurons in the upper and lower cortex at a specific location may not belong to the same column. Moreover, the bands of cells associated with a particular connection alternate with other bands of cells of approximately similar size and which have afferent or efferent connections with a different brain area [20]. Hence, NFT in the upper and lower cortical laminae of a particular gyrus could be associated with different cortico-cortical connections. This pattern, however, would predict that the clusters of NFT in the upper cortex would be negatively correlated (out of phase) with those in the lower cortex, a pattern which was not observed. Hence, it is likely that the clustering of NFT in the cortex represents the spread of NFT independently in relation to the FF and FB circuits, and that in some gyri the result is a fortuitous spatial correlation in the upper and lower laminae.

In conclusion, NFT in gyri of the temporal lobe in AD exhibit a regularly repeating pattern of clusters in the upper and lower laminae, the size distribution and spacing of which is consistent with their development in relation to the FF and FB cortico-cortical pathways. It is likely that the distribution of NFT in the upper and lower cortex of the temporal lobe represents the spread of NFT in relation to the cortico-cortical pathways and that this spread occurs relatively independently in relation to the FF and FB pathways. The data provide less evidence that there is vertical spread of NFT across the cortex within columns of cells.

### Acknowledgements

The assistance of the Brain Bank, Institute of Psychiatry, London in providing tissue sections for this study is gratefully acknowledged.

## References


1. Armstrong RA. Is the clustering of neurofibrillary tangles in Alzheimer's patients related to the cells of origin of specific cortico-cortical projections? Neurosci Lett 1993; 160: 57-60.
2. Armstrong RA. The usefulness of spatial pattern analysis in understanding the pathogenesis of neurodegenerative disorders, with special reference to plaque formation in Alzheimer's disease. Neurodegen 1993; 2: 73-80.
3. Armstrong RA. Clustering patterns of neurofibrillary tangles in Alzheimer's disease. Alz Rep 1999; 2: 151-154.
4. Armstrong RA. Analysis of spatial patterns in histological sections of brain tissue using a method based on regression. J Neurosci Methods 2000; 95: 39-45.
5. Armstrong RA. Measuring the degree of spatial correlation between histological features in thin sections of brain tissue. Neuropathology 2003;23: 245-253.
6. Armstrong RA. Methods of studying the planar distribution of objects in histological sections of brain tissue. J Microsc 2006; 221: 153-158.
7. Armstrong RA. Classic beta-amyloid deposits cluster around large diameter blood vessels rather than capillaries in sporadic Alzheimer's disease. Curr Neurovasc Res 2006; 3: 289-294.
8. Armstrong RA. Plaques and tangles and the pathogenesis of Alzheimer's disease. Folia Neuropathol 2006; 44: 1-11.
9. Armstrong RA, Myers D, Smith CU. The relationship between the spatial pattern of senile plaques and neurofibrillary tangles in Alzheimer's disease. Neurosci Res Commun 1990; 7: 105-111.
10. Armstrong RA, Myers D, Smith CU. The spatial patterns of plaques and tangles in Alzheimer's disease do not support the 'Cascade Hypothesis'. Dementia 1993; 4: 16-20.
11. Armstrong RA, Myers D, Smith CU, Cairns N, Luthert PJ. Alzheimer's disease: The relationship between the density of senile plaques, neurofibrillary tangles and A4 protein in human patients. Neurosci Lett 1991; 123: 141-143.
12. Armstrong RA, Slaven A. Does the neurodegeneration of Alzheimer's disease spread between visual cortical regions B17 and B18 via the feedforward or feedback short cortico-cortical projections? Neurodegen 1994; 3: 191-196.
13. Armstrong RA, Wood L. Spatial pattern analysis of beta-amyloid (Abeta) `deposits in Alzheimer disease by linear regression. Alz Dis Assoc Dis 1996; 10: 40-45.
14. Braak H, Braak E, Kalus P. Alzheimer's disease: areal and laminar pathology in the occipital isocortex. Acta Neuropathol 1989; 77: 494-506.
15. De Lacoste MC, White CL 3rd. The role of cortical connectivity in Alzheimer's disease pathogenesis: a review and model system. Neurobiol Aging 1993; 14: 1-16.
16. Fitzpatrick KA, Imig TJ. Auditory cortico-cortical connections in the owl monkey. J Comp Neurol 1980; 192: 589-610.
17. Friedman DP. Laminar patterns of termination of cortico-cortico afferents in the somatosensory system. Brain Res 1983; 273: 147-151.
18. Gallyas F. Silver staining of Alzheimer's neurofibrillary changes by means of physical development. Acta Morphol Acad Sci Hung 1971; 19: 1-8.
19. Hardy JA, Higgins GA. Alzheimer's disease: the amyloid cascade hypothesis. Science 1992; 256: 184-185.
20. Hiorns RW, Neal JW, Pearson RC, Powell TP. Clustering of ipsilateral cortico-cortico projection neurons to area 7 in the rhesus monkey. Proc R Soc Lond 1991; 246: 1-9.
21. Hof PR, Morrison JH. Quantitative analysis of a vulnerable subset of pyramidal neurons in Alzheimer's disease: 11 primary and secondary visual cortex. J Comp Neurol 1990; 301: 55-64.
22. Hyman BT, Van Hoesen GW, Wolozin BL, Davies P, Kromer LJ, Damasio AR. Alz-50 antibody recognizes Alzheimer-related neuronal changes. Ann Neurol 1988; 23: 371-379.
23. Lewis DA, Campbell MJ, Terry RD, Morrison JH. Laminar and regional distributions of neurofibrillary tangles and neuritic plaques in Alzheimer's disease: a quantitative study of visual and auditory cortices. J Neurosci 1987; 6: 1799-1808.
24. Mountcastle VB. An organizing principle for cerebral function: The unit module and the distributed system. In: The neurosciences. Fourth Study Program. Schmitt FO, Worden FG (eds.). MIT press, Cambridge Mass., pp. 21-42.
25. Mirra, S, Heyman, A, McKeel, D, Sumi, S, Crain, B, Brownlee, L, Vogel, F, Hughes, J, van Belle, G, Berg, L. The consortium to establish a registry for Alzheimer's disease (CERAD). II. Standardization of the neuropathological assessment of Alzheimer's disease. Neurology 1991; 41: 479-486.
26. Pearson RC, Esiri MM, Hiorns RW, Wilcock GK, Powell TP. Anatomical correlates of the distribution of the pathological changes in the neocortex in Alzheimer'a disease. Proc Natl Acad Sci USA 1985; 82: 4531-4534.
27. Rogers J, Morrison JH. Quantitative morphology and regional and laminar distributions of senile plaques in Alzheimer's disease. J Neurosci 1985; 5: 2801-2808.
28. Saper CB, Wainer BH, German DC. Axonal and transneuronal transport in the transmission of neurological disease: potential role in system degenerations, including Alzheimer's disease. Neuroscience 1987; 23: 389-398.
29. Tierney M, Fisher R, Lewis A, Zorzitto M, Snow W, Reid D, Nieuwstraten P. The NINCDS-ADRDA Work Group criteria for the clinical diagnosis of probable Alzheimer's disease: a clinicopathologic study of 57 cases. Neurology 1988; 38: 359-364.
30. Ungerleider LG, Desimone R. Cortical connections of visual area MT in the macaque. J Comp Neurol 1986; 248: 190-222.